Surface Passivation of Bare Aluminum Nanoparticles Using Perfluoroalkyl Carboxylic Acids

R. Jason Jouet,*,† Andrea D. Warren,† David M. Rosenberg,† Victor J. Bellitto,† Kihong Park,‡ and Michael R. Zachariah‡

Indian Head Division-Naval Surface Warfare Center, Research and Technology Department, 101 Strauss Avenue, Indian Head, Maryland 20640, Center for NanoEnergetics Research (CNER), UMCP/NIST Co-Laboratory on NanoParticle Based Manufacturing and Metrology, University of Maryland and National Institute of Standards and Technology (NIST), 2125 Glenn L. Martin Hall and B360 Physics, College Park, Maryland 20742, and National Institute of Standards and Technology, Gaithersburg, Maryland 20877

Received October 4, 2004. Revised Manuscript Received January 25, 2005

Surface passivation of unpassivated Al nanoparticles has been realized using self-assembled monolayers (SAMs). Nanoscale Al particles were prepared in solution by catalytic decomposition of $H_3Al{\cdot}NMe_3$ or $H_3Al{\cdot}N(Me)Pyr$ by $Ti(O^iPr)_4$ and coated in situ using a perfluoroalkyl carboxylic acid SAM. Because the Al particles are prepared using wet chemistry techniques and coated in solution, they are free of oxygen passivation. This SAM coating passivates the aluminum and appears to prevent the oxidation of the particles in air and renders the composite material, to some extent, soluble in polar organic solvents such as diethyl ether. Characterization data including scanning electron microscopy , transmission electron microscopy, thermogravimetric analysis, and attenuated total reflectance-Fourier transform infrared spectroscopy of prepared materials are presented.

Introduction

Metallization of energetics, the addition of combustible metal powders to formulations, is a technique used to increase the energy output of explosives and propellants. The metal of choice is aluminum because of its energy density due to the high relative heat of formation of the oxide, Al_2O_3. The energy density for the oxidation of aluminum is −7.4 kcal/g of Al ($\Delta H_f°(Al_2O_3) = -400.5$ kcal/mol).[1] By comparison, ϵ-CL-20, or hexaazahexanitroisowurzitane,[2] has a $\Delta H_{combustion} = -1.96$ kcal/g.[3] Boron is an obvious choice as an additive because of its energy density (oxidation of B to B_2O_3 releases 13.9 kcal/g); however, the presence of the low-melting oxide on the particle surface and the formation of HOBO intermediate species slow the combustion, reducing the rate of energy release. Comprehensive reviews of experimental and theoretical research findings of boron oxidation can be found in refs 4−6.

The addition of Al to a material typically requires the addition of an oxidizer, such as ammonium perchlorate (AP). The reaction of the metal with the oxidizer is an intermolecular reaction, which is to some extent diffusion-limited. In an attempt to reduce this diffusion limitation and increase the rate of Al oxidation so that the energy released can contribute to the detonation pressure and velocity, nanoscale Al particles are being employed. There are, however, significant drawbacks associated with the use of nanoscale aluminum particles for energetics applications.

Fundamentally the issue associated with all types of metallized energetic formulations is limited realization of the energy potential of the fuel. The two primary causes associated with this are incomplete Al combustion and excessive Al oxidation prior to combustion.

Incomplete combustion results principally from the formation of a thick oxide coating on the particle during the combustion event.[7] It has been proposed that oxygen diffusion into the Al particle is the primary means for combustion and that this diffusion is enhanced in local regions of the Al particle containing solid solutions of Al and O with high oxygen content.[7] This enhancement ultimately results in oxide cap formation which slows the combustion rate resulting in lower particle temperature.[7] Ultimately, the combustion process is prematurely terminated by excess oxide formation. This problem is somewhat mitigated with the use of nanoscale Al particles because they are small enough to combust completely before the oxide layer can prevent oxygen diffusion to the core.

Excessive oxidation prior to the combustion event is a concern when nanoscale or ultrafine Al (UFAl) is employed. The oxide coating thickness on an aluminum particle surface

* To whom correspondence should be addressed. E-mail: jouetrj@ih.navy.mil.
† Naval Surface Warfare Center.
‡ University of Maryland and NIST.

(1) Lide, D. R., Ed. *CRC Handbook of Chemistry and Physics,* 71st ed.; CRC Press: Boca Raton, FL, 1991.
(2) Nielsen, A. Polycyclic Amine Chemistry. In *Chemistry of Energetic Materials*; Olah, G. A., Squire, D. R., Eds.; Academic Press: San Diego, CA, 1991; pp 95−124.
(3) Simpson, R. L.; Urtiew, P. A.; Ornellas, D. L.; Moody, G. L.; Scribner, K. J.; Hoffman, D. M. *Propellants, Explos., Pyrotech.* **1997**, *22*, 249.
(4) Yeh, C. L.; Kuo, K. K. *Prog. Energy Combust. Sci.* **1996**, *22*, 511.
(5) Faeth, G. M. *21st JANNAF Combustion Meeting*, CPIA Vol. 1; Chemical Propulsion Information Agency: Columbia, MD, 1984; pp 15−29.
(6) King, M. K. In *Combustion of Boron-Based Solid Propellants and Solid Fuels*; Kuo, K. K., Pein, R., Eds.; Begell House and CRC Press Inc.: New York, NY, and Boca Raton, FL, 1993; pp 1−80.
(7) Dreizin, E. L. *Combust. Flame* **1999**, *117*, 841, and references therein.

10.1021/cm048264y CCC: $30.25
Published on Web 00/00/0000 PAGE EST: 10

can range between 1.7 and as much as 6.0 nm.[8] In the case of conventional micrometer-sized aluminum particles, this corresponds to approximately ≤0.5% of the total particle mass and is therefore not a significant reduction in reactive Al. As Al particle size is reduced, however, this oxide coating begins to represent a significant portion of the mass of the particle. In cases where the particles are very small, <50 nm, the oxide can represent 60% of the mass or more. Currently, there does not exist a means for the preparation of air-stable UFAl without this oxide coating.

Another obstacle associated with the use of UFAl is its processability. Typically metallized energetic formulations are composed of between 10 and 40% Al by mass with binder, high explosive, oxidizer, and plasticizers making up the bulk of the other components. Processing difficulties are experienced with UFAl because of its extremely high surface area. The binder(s) is simply, in some cases, incapable of wetting all of the solids. The result can be a crumbly, fragile material unsuitable for use.

Finally, a convenient method for large-scale production of UFAl does not currently exist. It is prepared expensively in batches by vapor condensation techniques and subject to oxidation/passivation before use. UFAL has a limited shelf life in that particle oxidation continues even after the outer layer is completely oxidized. This continued oxidation occurs because the Al_2O_3 coating is somewhat porous to oxygen, allowing further oxidation of the inner core during prolonged exposure—a phenomenon known as aging.

Surface functionalization of aluminum oxide surfaces has been demonstrated using silanols,[9] hydroxamic acids,[10] and carboxylic acids,[11] among others. Surface functionalization of oxide-free aluminum surfaces has been demonstrated using aldehydes[12] and formic acid.[13] Additionally, the interaction of Al atoms and carboxylate species was analyzed in detail by deposition of Al atoms onto a carboxy-terminated self-assembled monolayer (SAM) on Au.[14] Perfluorinated carboxylic acids have been used to stabilize the formation of Ag nanoparticles from thermal degradation of layered silver perfluorocarboxylates.[15] This research builds upon these results by using long-chain perfluorinated carboxylic acids as the surface-binding moiety for use in the functionalization of *unpassivated* Al nanoparticles (nanoAl). The resulting particle composites are thus comprised of an Al center core with covalently bonded perfluorinated alkyl species coating the outer surface. The presence of the perfluoroorganic carboxylate protects the Al nanoparticles from continued oxidation associated with aging in air, as well as improving particle−solvent interactions.

Experimental Section

General Considerations. All manipulations of air- and moisture-sensitive materials were performed in an Innovative Technologies System One-M glovebox containing an argon atmosphere or by standard Schlenk techniques. Dry toluene, diethyl ether perfluorotetradecanoic acid ($C_{13}F_{27}COOH$), perfluorononanoic acid ($C_8F_{19}COOH$), perfluoroundecanoic acid ($C_{10}F_{21}COOH$), titanium(IV) isopropoxide ($Ti(O^iPr)_4$), LAH, NMe_3·HCl, and methylpyrrolidine−alane adduct (H_3Al·N(Me)Pyr) were purchased from Aldrich Chemical. All materials were used as received except NMe_3·HCl, which was sublimed prior to use.

H_3Al·NMe_3. A typical reaction was conducted by adding dry NMe_3·HCl to a slurry of LAH in diethyl ether. This addition was conducted at room temperature, and the solution was allowed to stir for 12 h. The resulting gray slurry was then filtered, washed with diethyl ether, and the solid discarded. The wash was collected with the filtrate and this final solution was concentrated to dryness in vacuo. The resulting white solid was sublimed and stored in diethyl ether in the glovebox. The concentration of the solution with respect to Al was obtained gravimetrically by taking several aliquots of solution, decomposing the alane adduct to Al^0, removing the solvent, and weighing the product.

NanoAl/SAM Composite Material. *H_3Al·NMe_3 Decomposition−Al/$C_{13}F_{27}COOH$ Preparation.* A 0.26 M diethyl ether solution of H_3Al·NMe_3 (25 mL, 0.0065 mol) was stirred at room temperature in an argon-filled glovebox. To this solution, 16 μL of $Ti(O^iPr)_4$ in 1.6 mL of toluene was rapidly added via syringe. The reaction was stirred for 5 min, during which time the solution became dark brown in color. After 5 min, a solution of 0.94 g (0.0013 mol) $C_{13}F_{27}COOH$ in 25 mL of diethyl ether was added dropwise to the reaction flask at a rate of 3−4 drops/s. The reaction was stirred overnight, after which stirring was stopped and the reaction contents were allowed to settle. The clear brown ether layer was removed by pipet from the brown solid precipitate. The solid material was washed twice with 20-mL portions of diethyl ether. The solid was dried by allowing the residual ether to evaporate in the glovebox. The resulting dark gray, coated Al powder was found to be stable in air in that it was not pyrophoric and its appearance did not change with storage under ambient conditions. Yield: 0.80 g; (1.12 g (calc)); 71.4%.

H_3Al·N(Me)Pyr Decomposition−Al/$C_{13}F_{27}COOH$ Preparation. The following procedure is an example of the typical method used to form the nanoAl/SAM composite materials. A solution of diethyl ether (40 mL) and H_3Al·N(Me)Pyr (8.99 g, 0.0781 mol) was stirred at room temperature in a glovebox. To this solution, 120 μL of $Ti(O^iPr)_4$ was added rapidly via syringe. The reaction was stirred for 2 h, during which time the solution transitioned from dark brown upon $Ti(O^iPr)_4$ addition to black to dark gray. Following this decomposition, a solution of 11.15 g (0.0156 mol) $C_{13}F_{27}COOH$ in 30 mL of diethyl ether was added dropwise to the reaction flask at a rate of 3−4 drops/s. The reaction was stirred overnight, after which stirring was stopped and the reaction contents were allowed to settle. The clear brown ether layer was removed by pipet from the brown solid precipitate. The solid material was washed twice with 30-mL portions of diethyl ether. The solid was dried by

(8) Pesiri, D.; Aumann, C. E.; Bilger, L.; Booth, D.; Carpenter, R. D.; Dye, R.; O'Neill, E.; Shelton, D.; Walter, K. C.. *J. Pyrotech.* **2004**, *19*, 19.
(9) Sagiv, J. *J . Am. Chem. Soc.* **1980**, *102*, 92. Netzer L.; Sagiv, J. *J. Am. Chem. Soc.* **1983**, *105*, 674. Moaz, R.; Sagiv, J. *J. Colloid Interface Sci.* **1984**, *100,* 465. Houssiau, L.; Bertrand, P. *App. Surf. Sci.* **2001**, *175*, 351.
(10) Folkers, J. P.; Gorman, C. B.; Laibinis, P. E.; Buchholz, S.; Whitesides, G. M. *Langmuir* **1995**, *11*, 813.
(11) Karaman, M. E.; Antelmi; D. A.; Pashley, R. M. *Colloids Surf., A* **2001**, *182*, 285. Allara, D. L.; Nuzzo, R. G. *Langmuir* **1985**, *1,* 45, 52. Tao. Y. *J. Am. Chem. Soc***. 1993**, *115*, 4350. Tao, Y.; Hietpas, G. D.; Allara, D. L. *J. Am. Chem. Soc.* **1996**, *118*, 6724, and references therein. For reviews, see: Bain, C. D.; Whitesides, G. M. *Angew. Chem., Int. Ed. Engl.* **1989**, *28*, 506. Whitesides, G. M.; Laibinis, P. E. *Langmuir* **1990**, *6*, 87. Ulman, A. *An. Introduction to Ultrathin Organic Films from Langmuir−Blodgett to Self-Assembly*; Academic Press: San Diego, CA, 1991; Chapter 3.
(12) Sardar, S. A.; Duschek, R.; Blyth, R. I. R.; Netzer, F. P.; Ramsey, M. G. *Surf. Sci.* **2000**, *468*, 10.
(13) Crowell, J. E.; Chen, J. G.; Yates, J. T., Jr. *J. Chem. Phys.* **1986**, *85*, 3111.
(14) Fisher, G. L.; Hooper, A. E.; Opila, R. L.; Allara, D. L.; Winograd, N. *J. Phys. Chem. B* **2000**, *104*, 3267.
(15) Lee, S. J.; Han, S. W.; Kim, K. *Chem. Commun.* **2002**, 442.

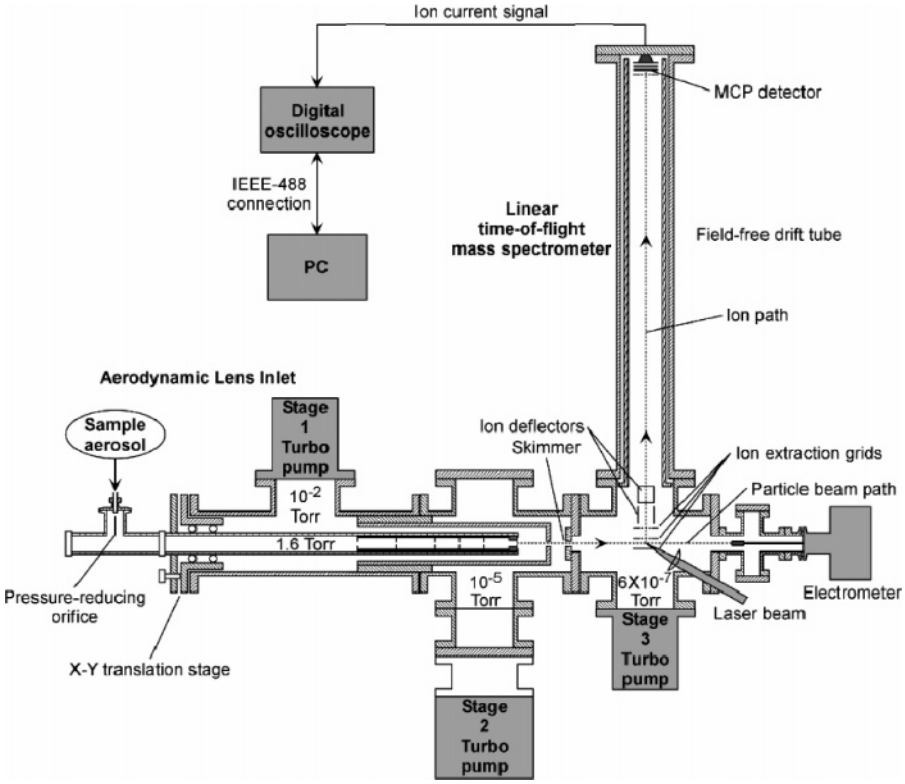

Figure 1. Schematic of single-particle mass spectrometer (SPMS).

allowing the residual ether to evaporate in the glovebox. The resulting dark gray, coated Al powder was found to be stable in air in that it was not pyrophoric and its appearance did not change with storage under ambient conditions. Yield: 13.0 g (13.26 g (calc)); 98.0%.

Thermogravimetric Analysis. Thermogravimetric analysis (TGA) experiments were conducted on a TA Instruments 2950 TG analyzer. The sample was run in an open Pt crucible under static air conditions. The heating profile was isothermal at 30 °C for 36 h and then ramped in HTGA mode at 20 °C/min.

SEM/EDAX. Scanning electron microscopy (SEM) and energy-dispersive X-ray analyses (EDAX) were conducted using a LEO 1550 scanning electron microscope operating in the InLens detector mode.

TEM. Transmission electron microscopy (TEM) was performed by Dr. Karl Martin at Nanotechnologies, Inc. using a JEOL 1200 EX instrument. The $AlC_{13}F_{27}COOH$ material was dispersed in methanol for placement on the grid.

Active Al Content, Base Hydrolysis Method. The active aluminum content of the material was determined by digesting a known amount in NaOH and measuring the volume of hydrogen gas evolved according to the procedure described in the literature.[16]

ATR−IR Measurements. Infrared spectra were obtained with a Nicolet 750 Magna FT-IR spectrometer equipped with a mercury−cadmium telluride (MCT-B) detector. The IR data were collected in attenuated total reflectance (ATR) mode using a Pike Technologies ATR accessory. The spectra are composed of 64 co-added sample scans of 1 cm^{-1} resolution in the range of 500−4000 cm^{-1} and were ratioed against 64 co-added background scans.

Single-Particle Mass Spectrometer Measurements. A single-particle mass spectrometer (SPMS) was used to determine the elemental composition of individual particles in real time.[17] As shown in Figure 1, the SPMS consists of an aerodynamic lens inlet, three-stage differential vacuum systems, a free firing pulsed laser for particle ionization, a linear time-of-flight mass spectrometer, and a 500-MHz digital oscilloscope and computer for data acquisition. The aerodynamic lens system produces a narrow collimated particle beam and transports particles of 30−300 nm into the high-vacuum system. The free firing pulsed laser (a frequency-doubled Nd:YAG laser operated at 10 Hz, 532 nm wavelength), through a spherical plano-convex lens, is tightly focused at the extraction field of the mass spectrometer and intersects the particle beam with a laser beam diameter of ∼0.3 mm and a laser pulse duration of ∼5 ns. The laser was operated with a laser energy power above ∼100 mJ/pulse to ensure complete particle ionization. The laser power density at the focal point was estimated to be approximately 1.7×10^{10} W/cm^2. The pressure of the mass spectrometer region is $\sim 10^{-7}$ Torr when the inlet is open. When the laser hits a particle successfully, all positive ions formed from the particle are accelerated along an ∼1-m time-of-flight tube and detected by microchannel plates (MCP). A photodiode sensor that detects laser firing was used to initiate the time-of-flight measurements. A 500-MHz digital oscilloscope selectively records time-of-flight spectra in which the intensity of the ion signal exceeds a certain level.

For single-particle analysis with the SPMS, coated aluminum nanoparticles need to be airborne. To do this, the $Al/C_{13}F_{27}COOH$ material in bulk samples was sonicated in methanol, and a collision atomizer was used to aerosolize the particles into argon gas from the solution. (Argon was used as a carrier gas so as to prevent Al_2O_3 formation during the thermal decomposition of the material at elevated temperatures.) The aerosolized particles passed through several driers to remove solvent from particles and then entered a tube furnace where particles endure high temperatures for a given residence time (∼1 s). A 120-cm quartz tube with a 1-cm inner diameter was placed in the tube furnace with a heated length of 30 cm. The aerosols from the tube furnace for the given temperature

(16) Fedotova, T. D.; Glotov, O. G.; Zarko, V. E *Propellants, Explos., Pyrotech.* **2000**, *25*, 325.

(17) Mahadevan, R.; Lee, D.; Sakurai, H.; Zachariah, M. R. *J. Phys. Chem. A* **2002**, *106,* 11083.

(25 to ~1100 °C) were directly sampled into the SPMS where their elemental composition can be determined as a function of the furnace temperature. In addition, a differential mobility analyzer (DMA) with the condensation particle counter (CPC) was used to measure the size distribution of aluminum nanopowders.[18]

Observations. Upon addition of the $Ti(O^iPr)_4$ to the $H_3Al{\cdot}NMe_3$/ether solutions a dark brown color was immediately observed. The vigorously bubbling solution then transitioned to black and, if left unattended, eventually gray and turbid. A mirror of Al was observed on the walls of the reaction flask. Addition of perfluorotetradecanoic acid ($C_{13}F_{27}COOH$), perfluorononanoic acid ($C_8F_{19}COOH$), or perfluoroundecanoic acid ($C_{10}F_{21}COOH$) prior to this point (usually when the solution appeared black but had not yet begun to deposit Al on the walls of the flask) prevents this agglomeration (grain growth) of aluminum particles.

The procedure using $H_3Al{\cdot}N(Me)Pyr$ as the Al source had to be altered to allow for complete alane decomposition. With addition of the $Ti(O^iPr)_4$, a dark brown color was again immediately observed. The solution then transitioned to a dark black color and eventually a gray turbid slurry. An Al mirror was not observed on the flask walls with use of $H_3Al{\cdot}N(Me)Pyr$. Additionally, less bubbling was observed during decomposition as compared to the $H_3Al{\cdot}NMe_3$, and the resulting particle appeared to be more finely dispersed.

For reactions involving perfluorotetradecanoic acid ($C_{13}F_{27}COOH$) or perfluoroundecanoic acid ($C_{10}F_{21}COOH$), after stirring the contents for 12 h and allowing the system to settle, voluminous brown material separated from the clear ether solution. Concentration to dryness of the clear ether solution and ether washes of the brown material left minute quantities of residual material that showed no C−F bonds by FTIR. Concentration of the brown voluminous material in vacuo or simply allowing the mother liquor to evaporate in the glovebox resulted in a dark brownish gray powder which could be suspended in diethyl ether.

For similar reactions involving perfluorononanoic acid ($C_8F_{19}COOH$), the results were markedly different. The final material in this case settled out during stirring and stuck to the walls of the flask as an intractable viscous brown gel which was insoluble in toluene, hexane, tetrahydrofuran (THF), and diethyl ether. Chlorinated solvents, such as dichloroethane, seemed to dissolve the material somewhat; however, evaporation to dryness yielded material with similar viscous tarlike properties. The material seemed unreactive in air, but due to foreseeable difficulties in processing, characterization of this material beyond SEM (Figure 2) and IR was abandoned. Figure 2a shows the peak that formed when the sample was smeared onto the SEM stage and the spatula was pulled upward. Figure 2b is the same sample at higher magnification, which shows the significant particle size distribution of the sample. Particles ranging from 30 to <300 nm are readily observable.

Discussion

Unpassivated nanoAl was prepared via modification of the method described by Higa and Johnson.[19] $H_3Al{\cdot}NMe_3$ was decomposed at room temperature in an argon-filled glovebox using a catalytic amount of $Ti(O^iPr)_4$ (solution in toluene). The reaction solvent in all cases was diethyl ether. This method is very efficient for the production of unpassivated nanoAl; however, if left unattended, the nanoAl particles will grow and agglomerate to form large spongy particles as well as coat the walls of the reaction vessel with a thin film of Al. Addition of the perfluorocarboxylic acid halts this process, and fine powders are produced.

The use of $H_3Al{\cdot}N(Me)Pyr$ in place of $H_3Al{\cdot}NMe_3$ seems to result in a slower decomposition process as the decomposition time had to be increased 200%. Additionally, formation of an Al mirror was not observed using this Al source. Presumably the N(Me)Pyr remains in solution in ether and acts as a capping agent for the bare Al surface retarding extensive agglomeration. The presence of N(Me)Pyr chemisorbed to the Ti^0 or Al^0 surface would slow the catalytic decomposition. Higa and Johnson investigated several adducting amines as solvents in their decomposition experiments and found that both the identity of the amine and its concentration had effect on the particle size obtained.[19]

Extensive experimentation was necessary to determine the proper ratio of carboxylic acid necessary to completely passivate the nanoAl. A ratio of 4.9 mol of Al to 1 mol of $C_nF_{2n+1}COOH$ was determined to be the minimum requirement of $C_nF_{2n+1}COOH$ necessary. Material obtained from reactions with a higher Al-to-acid ratio precipitated as particulate from solution, was very dark in color, and was *extremely* pyrophoric in air. The adequately passivated material formed from the nanoAl/$C_{13}F_{27}COOH$ reaction was not pyrophoric in air.

The active Al content of the Al/$C_{13}F_{27}COOH$ material was determined using base hydrolysis[16] to be 15.4% Al by mass. This is in excellent agreement with the calculated value based on reactant amounts of 15.9%.

The relatively low Al content is directly related to the particle size of the Al. Attempts at particle size control have been unsuccessful—temperature, catalyst/alane ratio, etc. In all cases reduction of the amount of carboxylic acid resulted in extremely pyrophoric material.

While the experimentally determined molar ratio of Al:organic of ~5:1 is promising, the mass ratio of the prepared materials is poor because of the low atomic weight of Al (26.98 g/mol) compared to the molecular weight of $C_{13}F_{27}COOH$ (714.12 g/mol). A perfluoroorganic acid was chosen as the SAM species for the oxidizing capacity of fluorine and the fact that formation of AlF_3 liberates 13.31 kcal/g of Al ($\Delta H_f°(AlF_3) = -359.5$ kcal/mol)[1] versus Al_2O_3, which releases 7.4 kcal/g of Al. On the basis of a fluorine oxidation of Al hypothesis, the optimum aluminum:perfluoroorganic ratio would be one that results in an aluminum:fluorine ratio of 1:3. However, more fuel-rich (higher Al content) materials may be desirable.

It is possible to estimate the theoretical size of the aluminum core from experimental results by considering the amount of acid required for passivation and the amount of aluminum prepared. As stated earlier, any deviation from the ratio of perfluoroacid to Al prepared in the direction of less acid resulted in extremely pyrophoric material. The most fuel rich ratio which produced air-stable material was 5:1 (Al:perfluoroacid, molar). This Al core estimation is accomplished by calculating the surface area per gram (SA/g) according to

$$\mathrm{SA}\ (\mathrm{m}^2/\mathrm{g}) = \frac{2\pi \mathrm{cr}_{\mathrm{Al}}{}^2 n_{\mathrm{C_{14F27O2H}}}}{m_{\mathrm{Al}}} \qquad (1)$$

(18) Knutson, E. O.; Whitby, E. R. *J. Aerosol Sci.* **1975**, *6*, 443.
(19) Higa; K. T.; Johnson; C. E.; Hollins; R. A. U. S. Pat. No. 5,885,321, 1999.

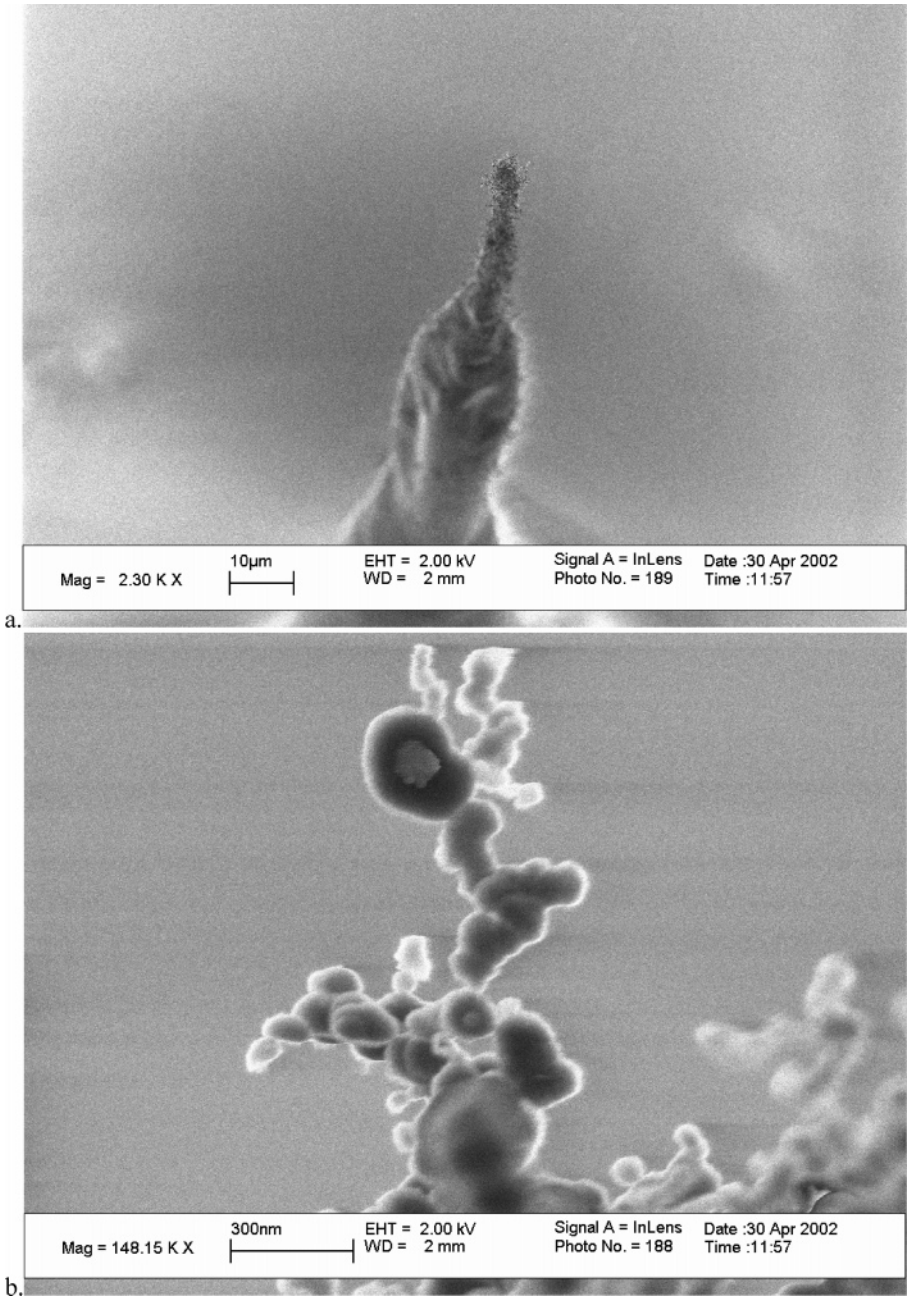

Figure 2. SEM images of the Al/$C_8F_{17}COOH$ composite at (a) 2K and (b) 148K magnification.

where cr_{Al} is the covalent radius of Al in meters, $n_{C_{13}F_{27}COOH}$ is the number of molecules of perfluoroacid, and m_{Al} is the mass of Al prepared experimentally. The assumptions made for this estimate are as follows: (1) the perfluoroacid coating is a monolayer, (2) each acid moiety binds to two different surface Al atoms, (3) the area occupied by an Al atom on the surface is equivalent to the surface area of a circle of diameter 2.5 Å (covalent radius of Al), and (4) all available Al is in the composite's core. Using this surface area value, the radius of a sphere of Al can be calculated using

$$\text{SA } (\text{m}^2/\text{g}) = \frac{4\pi r_p^{\,2}}{m_p} \qquad \text{where } m_p = {}^4/_3\pi r_p^{\,3}\rho_{Al}$$

$$r_p = \frac{3}{\text{SA}\rho_{Al}} \tag{2}$$

where r_p is the radius the particle in meters, m_p is the mass of the particle, and ρ_{Al} is the density of Al in g/m^3. From these calculations using experimental values of $C_{13}F_{27}COOH$ and $H_3Al{\cdot}N(Me)Pyr$, we estimate the Al core size to be approximately 5 nm.

TGA of the nanoAl/$C_{13}F_{27}COOH$ material showed a negligible weight gain after approximately 2200 min in air at 30 °C (Figure 3a). Subsequent heating of this material resulted in weight loss beginning at approximately 118 °C, with a rapid weight loss occurring at approximately 307 °C (Figure 3b). The final residual weight of the material was 19.9% of the original. Complete oxidation of the Al present in the sample should have resulted in a final mass of ca. 30% of the original. One possible explanation for this may be formation of volatile Al−F species during thermolysis which sublimed off during combustion of the material in air, resulting in a lower than predicted final mass.

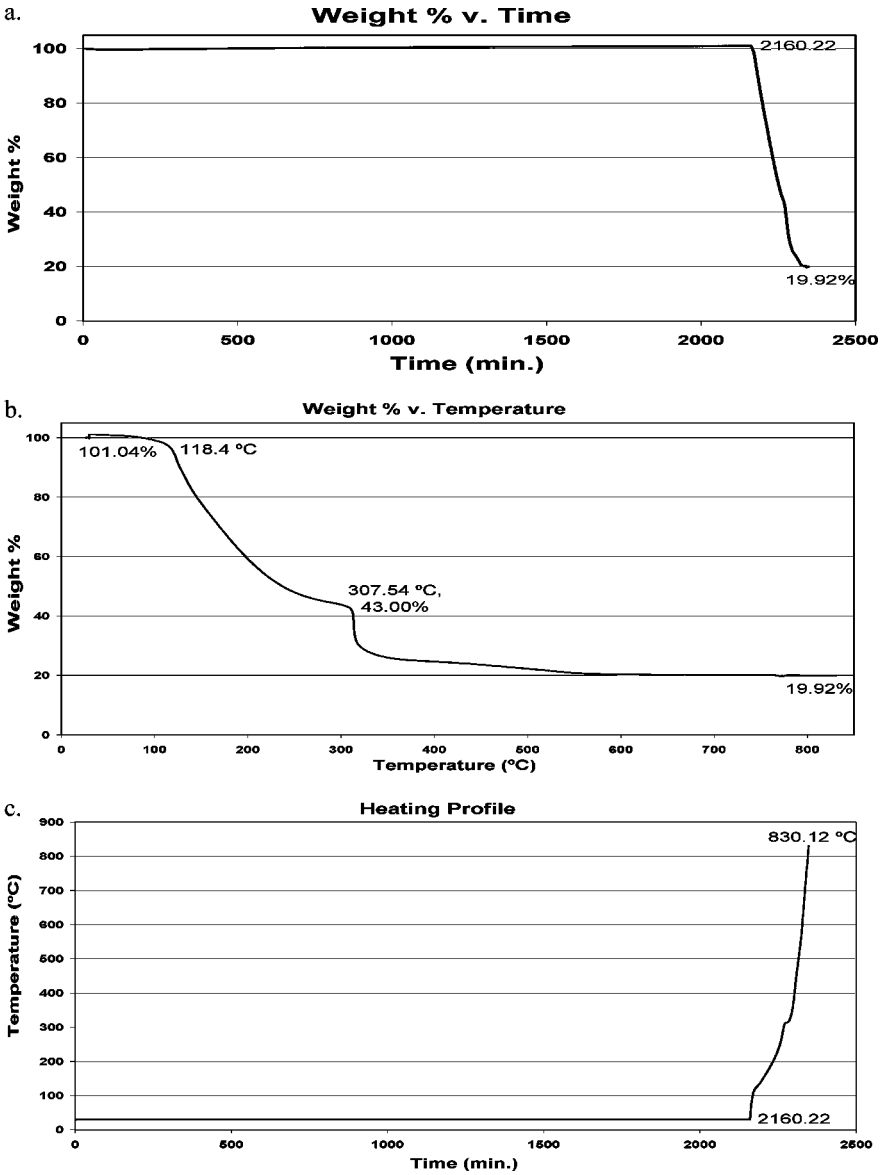

Figure 3. Thermogravimetric analysis of the Al/$C_{13}F_{27}COOH$ composite showing (a) the stability of the material in air, weight vs time; (b) thermal decomposition/combustion in air, weight vs time; and (c) the heating profile of the experiment, temperature vs time.

Scanning electron microscopy of the nanoAl/$C_{13}F_{27}COOH$ composite was limited in that intense magnification resulted in sample charging and image degradation. Additionally, under extreme magnification, the particles became so highly charged that repulsion-induced movement or charge-initiated chemical reaction appeared to have taken place. Acceptable images were obtained (Figure 4) at 200 K and less magnification. It is clear from these images that the material contains structures on the order of 50−100 nm in size. Whether the material is highly agglomerated in nature or not is indeterminate.

SEM images of the nanoAl/$C_8F_{17}COOH$ composite are presented in Figure 2. This material was essentially featureless at all available magnifications. As this material was a gel, SEM analysis required that it be smeared onto the SEM stage. The interesting image in Figure 2a is the peak structure that remained when the spatula used to apply the composite was pulled from the stage. Figure 2b is a portion of this peak at 148 K magnification and demonstrates particle morphology despite the fact that the bulk material appeared as a gel.

The energy-dispersive spectroscopy (EDAX) analysis of the nanoAl/$C_{13}F_{27}COOH$ composite is presented in Figure 5; the EDAX spectrum of nanoAl/$C_8F_{17}COOH$ is presented in Figure 6. In both cases the spectra indicate a high relative concentration of fluorine on the surface of the particles. The relative intensity of the peaks assigned to C and O are significantly lower than the peak assigned to Al. As the depth in a material to which EDAX probes is dependent on the accelerating voltage of the electrons, one can assume that the accelerating voltage of 17 kV used in the experiments was sufficient to probe into the particle core.

Infrared Spectroscopy Measurements. Figure 7a shows the ATR-FTIR spectrum of the perfluorotetradecanoic ($C_{13}F_{27}$-COOH) acid, and Figure 7b corresponds to the ATR-FTIR spectrum of nanoaluminum that was passivated with $C_{13}F_{27}COOH$. The 500−1375-cm^{-1} region is similar in appearance for both spectra except for differences in intensities. The 520−830-cm^{-1} region is associated with the C−F deformation modes, while the 1000−1360-cm^{-1} region is associated with the C−F stretching modes.[20,21] The similarity

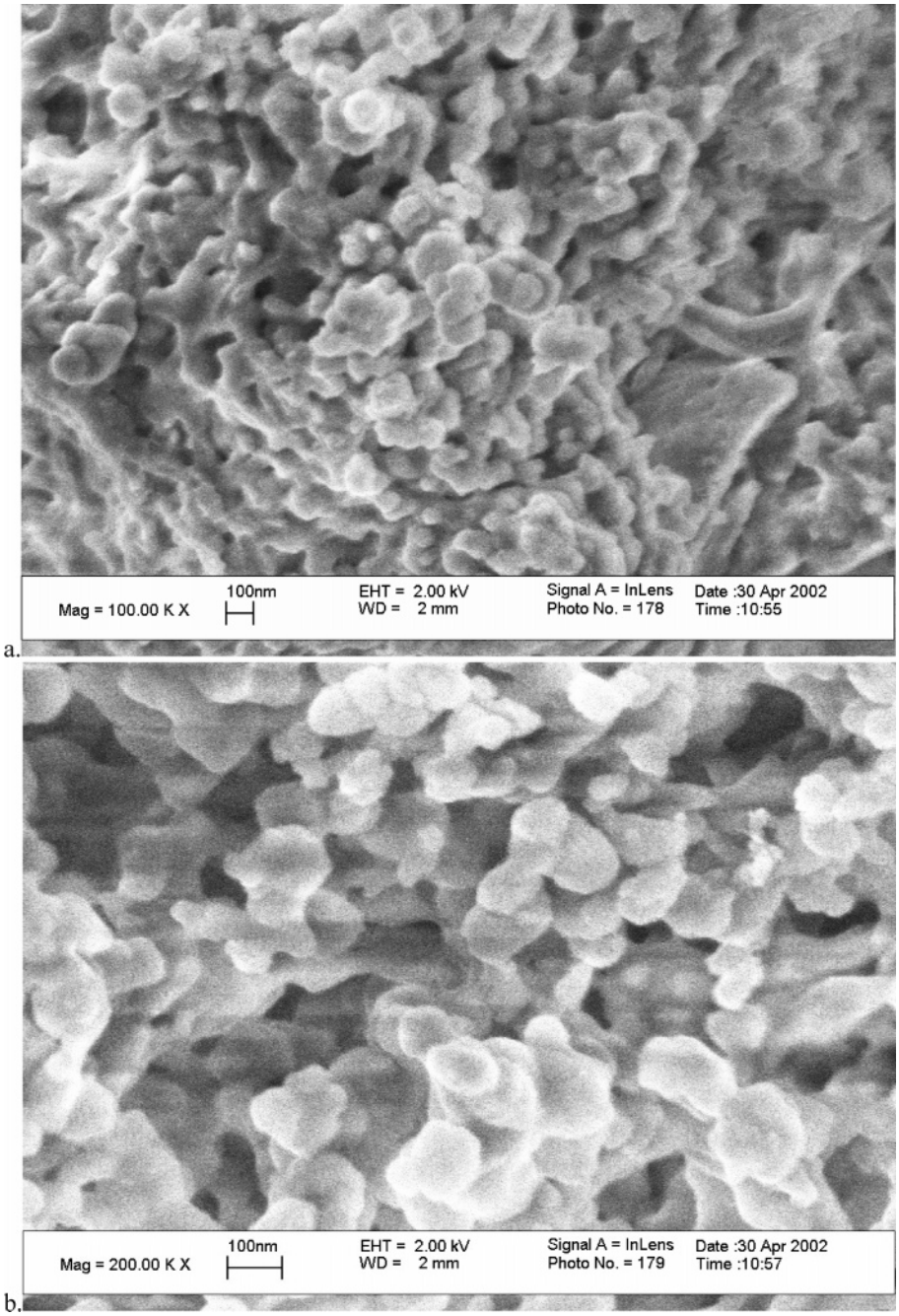

Figure 4. SEM images of the Al/$C_{13}F_{27}COOH$ composite at (a) 100K and (b) 200K magnification.

in appearance of the C−F regions suggests the C−F groups of $C_{13}F_{27}COOH$ remain intact upon adsorption to the nanoaluminum particles.

In polyfluorinated compounds, the modes associated with the C−F stretching vibrations are affected by neighboring atoms and are typically observed over a broad frequency range of 1000−1360 cm^{-1}.[20] Kim et al. showed through density functional theory calculations for fluorobutyl moieties that there is strong coupling of the C−F and C−C modes which make it difficult to assign any observed frequency to specific functional groups.[21] Therefore, the observed frequencies that may be associated with C−F and C−C groups are difficult to assign to specific modes since both the C−F stretching and bending modes lie in a region where strong coupling occurs with the C−C skeletal modes.

Comparison of the spectra in the 1400−3500-cm^{-1} region indicates considerable differences. The most notable is the absence of the carbonyl (C═O) stretching mode at 1754 cm^{-1} and the O−H stretching modes at 2920 and 3076 cm^{-1} in the coated nanoaluminum. The lack of any carbonyl and O−H stretching modes in Figure 7b indicates that the carboxylic acid adsorbs to the nanoaluminum through scission of the O−H bond and consequently results in the formation of a carboxylate species. The additional modes at 1482 and 1667 cm^{-1} observed in the spectrum for the passivated nanoparticles are therefore assigned to the symmetric carboxylate (ν_s(COO)) and antisymmetric carboxylate (ν_a(COO)) stretching modes, respectively.

(20) Socrates, G *Infrared Characteristic Frequencies*, 2nd ed.; John Wiley & Sons: New York, 1994; p 155.
(21) Kim, C. S.; Mowrey, R. C.; Butler, J. E.; Russell, J. N., Jr. *J. Phys. Chem. B* **1998**, *102*, 9290.

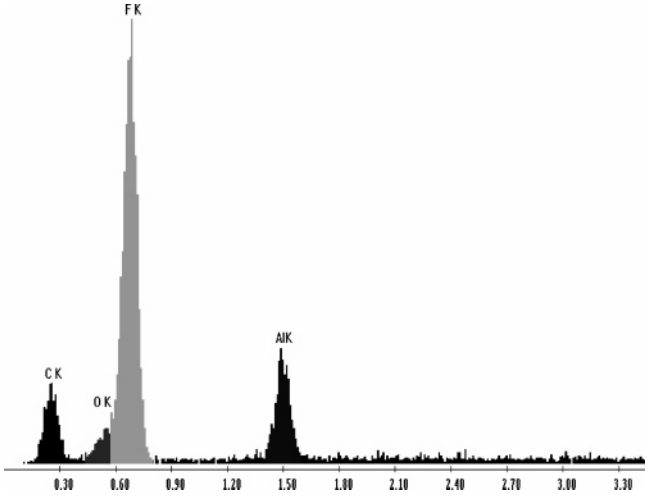

Figure 5. EDAX spectrum of the Al/$C_{13}F_{27}COOH$ composite showing relative intensities of X-ray emission peaks assigned to C, O, F, and Al.

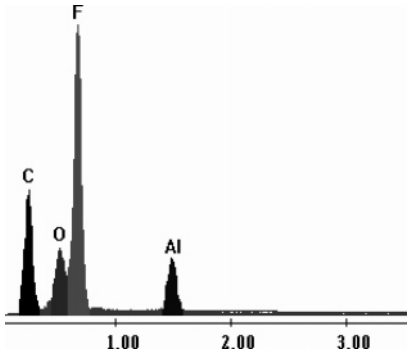

Figure 6. EDAX spectrum of the Al/$C_8F_{17}COOH$ composite showing relative intensities of X-ray emission peaks assigned to C, O, F, and Al.

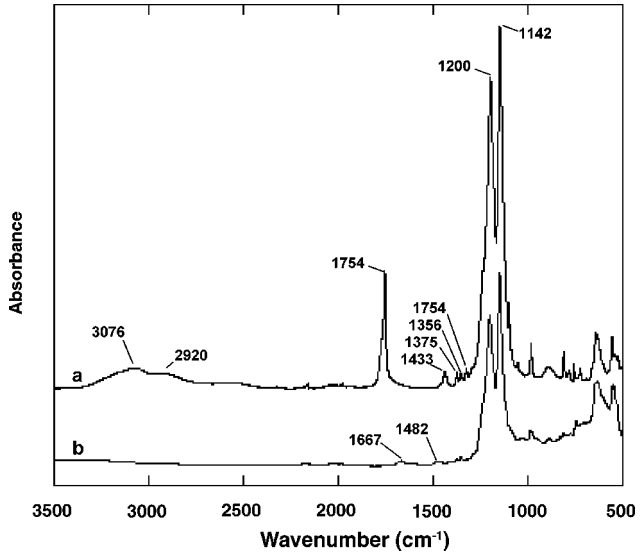

Figure 7. ATR-FTIR spectrum of the free perfluorotetradecanoic ($C_{13}F_{27}COOH$) acid (a) and the Al/$C_{13}F_{27}COOH$ composite material (b).

There are three distinct types of coordination that the carboxylate group can adopt for bonding to the Al surface. Shown in Figure 8 are the three proposed structures of the monodentate, bidentate, and bridging coordination types. In the monodentate geometry, only one oxygen atom is bonded to the aluminum surface. For the bidentate coordination, the oxygen atoms are both bonded to the same aluminum atom.

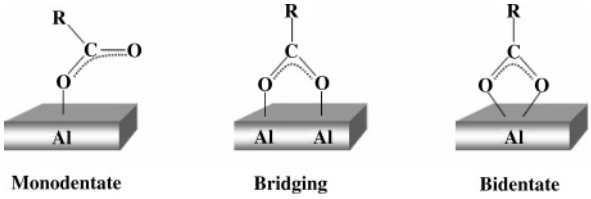

Figure 8. Three proposed structures for carboxylate binding to Al surface. In the monodentate geometry only one oxygen atom is bonded to the aluminum surface. For the bidentate coordination, the oxygen atoms are both bonded to the same aluminum atom. In the bridge-bonded configuration, the oxygen atoms are identical but on different aluminum atoms.

In the bridge-bonded configuration, the oxygen atoms are identical but on different aluminum atoms. It has been observed that the separation between the ν_s(COO) and ν_a(COO) modes can be used to determine the bonding geometry of the carboxylate species with the metal surface.[13,22,23] Deacon et al. assigned the bonding geometry from a survey of compounds formed between the carboxylate species and metals.[22] Frequency differences of $\sim$200 cm^{-1} are attributed to a bridging geometry, while differences of $\leq$80 cm^{-1} are attributed to a bidentate bonding arrangement, and differences of $\sim$300 cm^{-1} are associated with a monodentate bonding geometry. The frequency difference of 185 cm^{-1} [ν_a(COO) $-$ ν_s(COO)] observed in Figure 7b for the nanoaluminum particles coated with the carboxylic acid indicates that the carboxylate species that is formed is bridge-bonded to two aluminum atoms. This result is similar to that of Crowell et al. who studied the adsorption of formic acid[13] and acetic acid[23] on the Al(111) surface using high-resolution electron-energy-loss spectroscopy and found that both carboxylates bond in a symmetric bridging geometry.

Although the IR spectra were obtained in ambient air, the coated nanoaluminum particles appear to be oxide-free. The spectrum of the coated nanoaluminum does not exhibit features that are characteristic of any O_2 chemisorption or oxidic formation. Zhukov et al. investigated the oxygen adsorption on the Al(111) surface using high-resolution electron-energy-loss and X-ray photoelectron spectroscopies and demonstrated that vibrational modes at $\sim$610 and $\sim$825$-$865 cm^{-1} are indicative of an oxide formation, whereas a mode at $\sim$590 cm^{-1} is indicative of chemisorbed oxygen.[24]

A TEM image of Al/$C_{13}F_{27}COOH$ is shown in Figure 9. The particles appear to range in size from approximately 20 to 150 nm. They were dispersed in methanol prior to being placed on the grid; however, there is still significant clumping of the powder. Close inspection of the individual particles in the image reveals that several appear to have grown together.

Single-Particle Mass Spectrometer. Experiments were conducted using the SPMS and differential mobility analyzer$-$condensation particle counter (DMA-CPC) to better determine the elemental composition, particle size, and thermal stability of the Al/ $C_{13}F_{27}COOH$ material.

(22) Deacon, G. B.; Phillips, R. J. *Coord. Chem. Rev.* **1980**, *33*, 227.
(23) Crowell, J. E.; Chen, J. G.; Yates, J. T., Jr. *J. Electron Spectrosc. Relat. Phenom.* **1986**, *39*, 97.
(24) Zhukov, V.; Popova, I.; Fomenko, V.; Yates, J. T., Jr. *Surf. Sci.* **1999**, *441*, 240.

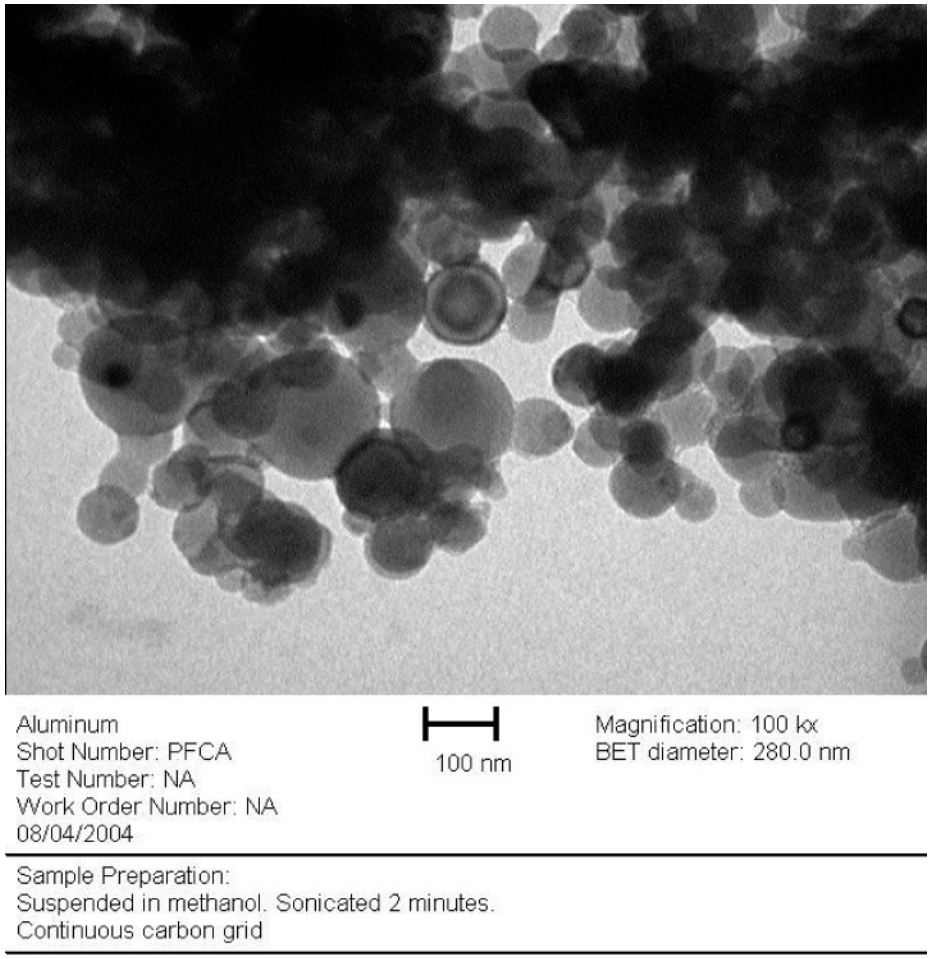

Figure 9. TEM image of Al/$C_{13}F_{27}COOH$ showing particles with sizes ranging from ~20 to ~150 nm.

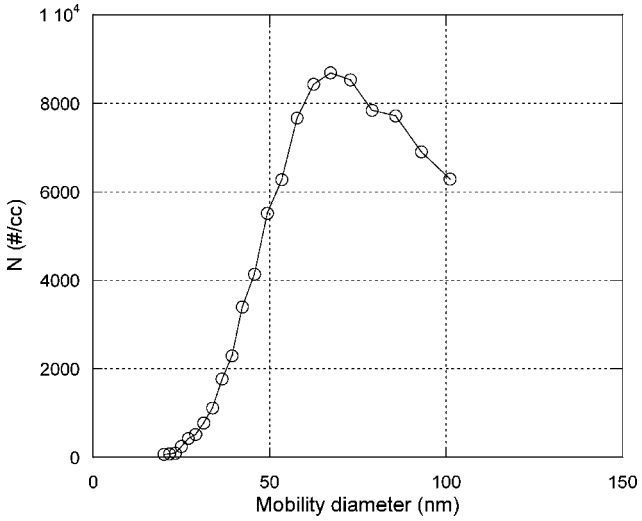

Figure 10. Size distribution of coated aluminum nanoparticles, Al/$C_{13}F_{27}COOH$, measured with the DMA-CPC.

The size distribution of coated aluminum particles measured with the DMA-CPC is shown in Figure 10. The peak size that gives the highest number concentration is 67 nm. Note that the size used here is the mobility equivalent diameter.

Examples of mass spectra for two types of aluminum nanoparticles measured with the SPMS are shown in Figure 11. Detection of C, F, O, and H in the single-particle mass spectrum as shown in Figure 11a suggests that the aluminum particles are coated with perfluoroalkyl species. Figure 11b shows the mass spectrum for a particle containing only Al, suggesting this particle is pure aluminum. Note that since argon was used as a carrier gas, oxidation of aluminum was mitigated. To examine the thermal stability of this coated material under elevated temperatures and to determine the relative amount of coated aluminum particles, we collected at least 200 mass spectra at each temperature, 25, 200, 400, 600, and 800 °C, and quantitatively determined the fraction of coated or uncoated aluminum particles. These results are plotted in Figure 12. As the furnace temperature increased, the fraction of particles containing Al, C, F, O, and H significantly decreased, while the fraction of particles containing only Al increased (i.e., the coating species would be desorbed off from the aluminum particle with increasing temperature, leading to the increase of the fraction of pure aluminum particles). However, it was observed that only 42% of the particles contained Al, C, F, O, and H (i.e., coated aluminum particles) at 25 °C. This is likely due to material degradation during aerosolization in methanol. Not shown, we did observe soot particles (i.e., particles containing C and H without Al) and aluminum particles containing only C above 1000 °C, suggesting that vapors from solvents (ether or methanol) used here contributed to the formation of soot and aluminum carbide particles at temperatures above 1000 °C.

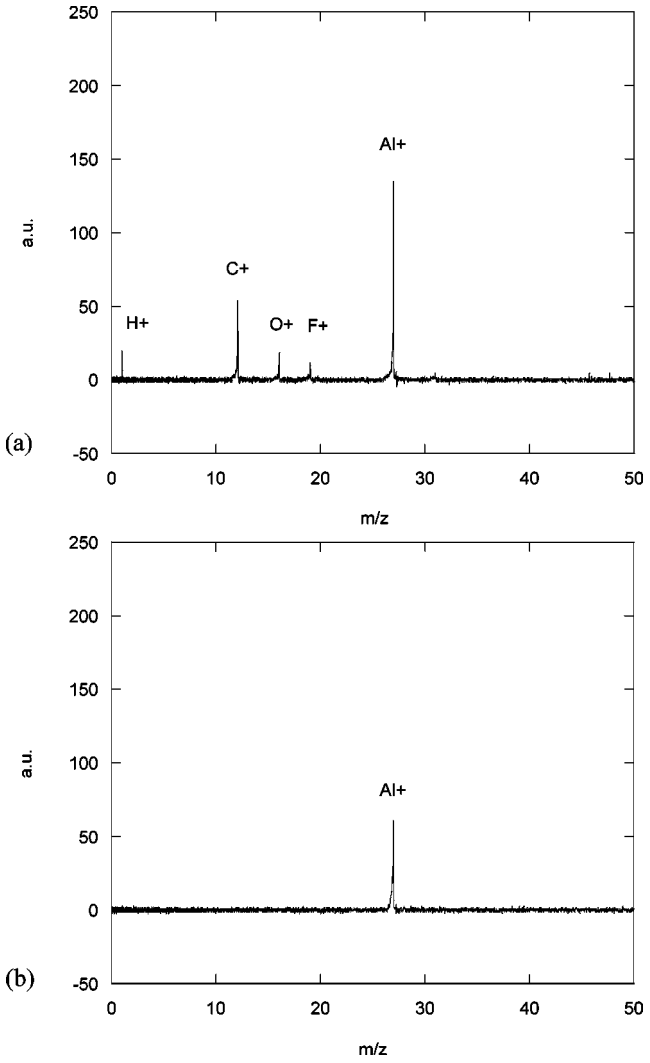

Figure 11. Typical mass spectra for (a) Al/$C_{13}F_{27}COOH$ particles and (b) pure aluminum nanoparticles measured with SPMS at 25 °C.

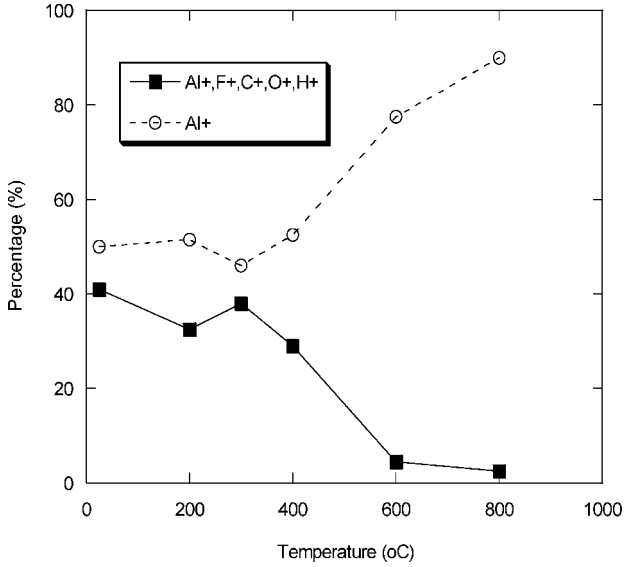

Figure 12. Fraction of two types of aluminum particles (i.e., coated aluminum particles and pure aluminum particles) as a function of temperature.

Conclusions

The solution-phase nanoAl preparation and in situ passivation with perfluorocarboxylic acids results in perfluoro-organic coated, oxide-free Al nanoparticles. Because the nanoAl is prepared under solvent (dry ether) in an argon-filled glovebox, the chance of adventitious oxidation or nitridation is greatly reduced relative to gas condensation or mechanical attrition means of nanoAl preparation.[25] Additionally, the continued nucleation (grain growth) of the prepared nanoAl is arrested by the addition of perfluorocarboxylic acid. The acid reacts with nanoAl, releasing H_2 and forming a protective layer on the particle. The cessation of Al grain growth upon perfluorocarboxylic acid addition effectively demonstrates the hypothesis proposed by Haber and Buhro[25] that nanoAl grains can be kinetically stabilized and the growth halted by "extrinsic impurities"—in this case, perfluorocarboxylic acid.

The prepared material composites are stable with respect to oxidation in air and have promising solvent interactions which should help with incorporation into energetic formulations. Additionally, the final material properties seem to depend greatly on the passivating agent used. Passivation of nanoAl using perfluorononanoic acid ($C_8F_{19}COOH$) results in a viscous tarlike final material, while the use of perfluorotetradecanoic acid ($C_{13}F_{27}COOH$) and perfluoroundecanoic acid ($C_{10}F_{21}COOH$) for passivation results in final materials which are powders that show appreciable solvent interaction.

The Al/$C_{13}F_{27}COOH$ material was analyzed for active Al content and found to be 15.4%. This is far below the active Al content of common nanoscale Al particles. We are currently investigating alternative means for preparing oxide-free Al nanoparticles for passivation using this technology with the goal of increasing the Al core size and thus making a more fuel rich material. It is believed that the energy content of current and future explosive and propellant formulations can be increased by elimination of the parasitic oxide present on conventional Al as well as utilization of fluorine as the oxidizer to make Al−F species. We believe that the energy release rate can be influenced by controlling the Al particle size as well as selection of the appropriate carboxylic acid passivating agent for the Al particles. The combination of oxidizer moieties in molecular proximity to Al particles has the potential for extremely fast Al oxidation so that the energy released can actually participate in the detonation phenomenon. The controlled and sustained contribution of the energy from Al oxidation to the detonation wave would represent a dramatic increase in performance and would begin to bridge the gap between conventional chemical and nuclear systems.

Acknowledgment. Funding for this work was provided by the NSWCI−IHD In-House Laboratory Independent Research Program managed by Anh N. Duong. The authors are grateful to Dr. K Higa and C. Johnson of the Naval Air Warfare Center, China Lake, CA, for conducting base hydrolysis active Al content analysis and, more importantly, for many very helpful discussions related to this project. Dr. Karl Martin of Nanotechnologies, Inc., Austin, TX, graciously provided the TEM data presented in this work for which we are grateful.

CM048264Y

(25) Haber, J. A., Buhro, W. E. *J. Am. Chem. Soc.* **2003**, *120*, 10847.